

SAND REPORT

SAND2003-0115

Unlimited Release

Printed January, 2003

A Technique for Determining Non-Linear Circuit Parameters from Ring Down Data

Louis A. Romero, Fred M. Dickey, Holly Dison

Prepared by
Sandia National Laboratories
Albuquerque, New Mexico 87185 and Livermore, California 94550

Sandia is a multiprogram laboratory operated by Sandia Corporation,
a Lockheed Martin Company, for the United States Department of Energy's
National Nuclear Security Administration under Contract DE-AC04-94-AL85000.

Approved for public release; further dissemination unlimited.



Sandia National Laboratories

Issued by Sandia National Laboratories, operated for the United States Department of Energy by Sandia Corporation.

NOTICE: This report was prepared as an account of work sponsored by an agency of the United States Government. Neither the United States Government, nor any agency thereof, nor any of their employees, nor any of their contractors, subcontractors, or their employees, make any warranty, express or implied, or assume any legal liability or responsibility for the accuracy, completeness, or usefulness of any information, apparatus, product, or process disclosed, or represent that its use would not infringe privately owned rights. Reference herein to any specific commercial product, process, or service by trade name, trademark, manufacturer, or otherwise, does not necessarily constitute or imply its endorsement, recommendation, or favoring by the United States Government, any agency thereof, or any of their contractors or subcontractors. The views and opinions expressed herein do not necessarily state or reflect those of the United States Government, any agency thereof, or any of their contractors.

Printed in the United States of America. This report has been reproduced directly from the best available copy.

Available to DOE and DOE contractors from
U.S. Department of Energy
Office of Scientific and Technical Information
P.O. Box 62
Oak Ridge, TN 37831

Telephone: (865)576-8401
Facsimile: (865)576-5728
E-Mail: reports@adonis.osti.gov
Online ordering: <http://www.doe.gov/bridge>

Available to the public from
U.S. Department of Commerce
National Technical Information Service
5285 Port Royal Rd
Springfield, VA 22161

Telephone: (800)553-6847
Facsimile: (703)605-6900
E-Mail: orders@ntis.fedworld.gov
Online order: <http://www.ntis.gov/help/ordermethods.asp?loc=7-4-0#online>



SAND2003-0115
Unlimited Release
Printed January 2003

A Technique for Determining Non-Linear Circuit Parameters from Ring Down Data

Louis A. Romero
Computational Mathematics and Algorithms Department

Fred M. Dickey
Firing Set and Optical Engineering Department

Holly Dison
Computational Mathematics and Algorithms Department

Sandia National Laboratories
P.O. Box 5800
Albuquerque, NM 87185-1111

Abstract

We present a technique for determining non-linear resistances, capacitances, and inductances from ring down data in a non-linear RLC circuit. Although the governing differential equations are non-linear, we are able to solve this problem using linear least squares without doing any sort of non-linear iteration.

1 Introduction

In this paper we present a technique for determining the parameters in a nonlinear RLC circuit from ring down data. We begin by defining precisely what we mean by a ring down experiment. We suppose that we have charged up a capacitor to a voltage V_0 , and that at time $t = 0$ a switch is closed so that the capacitor discharges through an RLC circuit. We measure the current $I(t)$ from $t = 0$ to a time T that may or may not be large enough for the capacitor to discharge completely.

The charge on the capacitor is given by

$$Q(t) = Q_0 - \int_0^t I(s) ds$$

Requiring that the voltage drop across the loop vanishes implies that [1], [2]

$$\frac{d}{dt} (L(I)I) + R(I)I = \frac{Q}{C(Q)}$$

Here $L(I)$, $R(I)$, and $C(Q)$ are the nonlinear inductance, resistance, and capacitance. Using the relation $\frac{dQ}{dt} = -I(t)$ we get the second order differential equations

$$\frac{d}{dt} (L(I)I) + R(I)\dot{Q} + \frac{Q}{C(Q)} = 0 \quad (1a)$$

where

$$I = -\dot{Q} \quad (1b)$$

$$Q(0) = Q_0 \quad (1c)$$

$$\dot{Q}(0) = 0 \quad (1d)$$

Note that the charge Q_0 is not given as data in our ring down experiment, but must be determined as part of our fitting algorithm. The purpose of this paper is to present a technique for determining the functions $L(I)$, $R(I)$, and $C(Q)$ from a knowledge of the current $I(t)$ in this ring down experiment.

At first sight this appears to be a nonlinear curve fitting problem. However, we will show that by choosing the right optimization problem, we can estimate the nonlinear circuit parameters using linear least squares.

We will briefly summarize the conclusions of this work.

- When there is no noise present our technique allows us to accurately predict arbitrarily complicated functions I , $L(I)$, and $C(Q)$ from ring down data.
- In the presence of noise it becomes difficult to predict complicated functions, but we can predict general trends in these functions correctly.

We now give an outline of the rest of this paper. In section 2) we discuss the technique for determining the circuit parameters in a linear RLC circuit. We present this analysis separately since it illustrates the technique without getting into some of the technical difficulties associated with the non-linear RLC curve fitting problem. In section 3) we discuss a few of the numerical details associated with this algorithm. In section 4) we generalize this technique to non-linear RLC circuits. We give numerical examples in section 5) and conclusions in section 6).

2 Determining the Parameters in a Linear RLC Circuit

In this section we present the technique for the particular case of determining the parameters of a linear RLC circuit from ring down data. The charge $Q(t)$ in a linear RLC circuit [3] satisfies

$$L\ddot{Q} + R\dot{Q} + Q/C = 0 \text{ for } 0 < t < T$$

along with the initial conditions

$$Q(0) = V_0 C$$

$$\dot{Q}(0) = 0$$

We assume that we know the initial voltage V_0 , and that we have experimental data $I_e(t)$ that we would like to fit. Given the circuit parameters R , L and C , we can determine the current $I_{model}(R, L, C, t)$ by analytically or numerically integrating the differential equations. If we try to minimize the error

$$\int_0^T |I_{model}(R, L, C, t) - I_e(t)|^2 dt$$

we get a nonlinear least squares problem. We emphasize that this particular minimization problem gives a nonlinear least squares problem even for the case of linear circuit elements.

However, we now show how we can estimate the parameters R , L , and C using linear least squares. In order to do this we first write

$$Q^*(t) = - \int_0^t I(s) ds = Q(t) - Q_0 \tag{2}$$

Here Q_0 is the initial charge on the capacitor. If our ring down data includes enough data so that the capacitor has completely discharged, we can compute Q_0 using

$$Q(\infty) = Q_0 - \int_0^\infty I_e(t) dt = 0$$

This implies that

$$Q_0 = \int_0^\infty I_e(t) dt \quad (3)$$

If we assume that we can calculate Q_0 in this way, it simplifies our curve fitting problem; however, we will not make this assumption in our algorithm.

The function $Q^*(t)$ satisfies the equation

$$L\ddot{Q}^*(t) + R\dot{Q}^*(t) + Q^*/C = -V_0$$

In order to estimate R , L and C we assume that we have smoothed the data so that we have an analytical expression $I_{fit}(t)$ that approximates the data. This allows us to get analytical expressions for Q^* and its derivatives.

Assuming that we have fit the data $\ddot{Q}^*(t)$, $\dot{Q}^*(t)$, and $Q^*(t)$, we now solve the overdetermined linear system

$$L\ddot{Q}^*(t_j) + R\dot{Q}^*(t_j) + Q^*(t_j)/C = -V_0 \quad j = 0, N_{dat} \quad (4)$$

Here N_{dat} is the number of data points that we choose to impose the equation at. This gives us N_{dat} linear equations in three unknowns R , L , and C . In general N_{dat} will be much larger than 3, so we will have a highly overdetermined linear system of equations. We solve these equations in a least squares sense to get R , L and C . We emphasize that this fit does not minimize the mean square error between $I_{model}(R, L, C, t)$ and $I_{fit}(t)$, but instead minimizes the error in the differential equation. This simple change in the procedure has resulted in turning a nonlinear least squares problem into a linear one.

There are three basic steps in our procedure for determining R , L , and C .

- Get an analytical fit $I_{fit}(t)$ to the experimentally measured current $I_e(t)$.
- Process $I_{fit}(t)$ to get the functions \ddot{Q}^* , \dot{Q}^* , and Q^* .
- Given V_0 , and the function $Q^*(t)$ and its first two derivatives, solve the overdetermined set of linear equations in 4).

We illustrate our algorithm on a linear numerically generated example with $L = .1$, $R = .2$, and $C = 1$. Figure 1a) shows some ring down data generated with these parameters. When we apply our algorithm to this data we get back exactly the values for the RLC parameters that were used in generating the data. In order to get some feel for the performance of the algorithm in the presence of noise, we have added random noise to the data as in figure 1b) (2.5 percent of the peak value). Although this type of high frequency random noise is not necessarily characteristic of the noise present in real ring down data, we see that after smoothing this data we get some data as in figure 1c) that has low frequency noise on it. When we fit this smoothed data we get values of $R = .177$, $L = .0975$, and $C = 1.152$. These are fairly reasonable values of the

parameters considering the level of noise that has been added to the data. In figure 1d) we see the current generated by these values of the RLC parameters. We see that there is quite significant error in the current generated by these parameters, even though the parameters themselves are quite good. We believe that this example shows that the algorithm works quite well for linear circuits even in the presence of noise.

3 Some Details of Implementation

In principle the procedure we outlined in the last section is quite simple. However, if the algorithm is implemented too crudely, it can result in some serious numerical difficulties

The first detail involves the scaling of the data. Typically our experimental data $I_e(t)$ is expressed in terms of seconds. If the time scale for discharging the circuit is very small (or large) when expressed in terms of seconds, this will result in the overdetermined system of equations in 4) having a large condition number. This can lead to large roundoff errors when doing the computations, and will result in good software packages giving error messages. This can be avoided by merely redefining the unit of time. When we redefine the unit of time, we end up changing the units of the R , L , and C . We suggest that the calculations be carried out using scaled versions of t , R , L , and C , and then converting the final answers back to the unscaled form. We now illustrate the process of scaling the data.

Suppose that we introduce a characteristic time scale T^* . This does not have to be chosen precisely, it is just a unit of time other than seconds that we would like to express our times in. We could for example choose T^* to be one millisecond, or a microsecond, or the approximate time for the capacitor to discharge. We now introduce the scaled time s defined by

$$s = t/T^*$$

In terms of s we have the scaled current

$$I_{scaled}(s) = I_e(sT^*),$$

and the scaled charge

$$Q_{scaled}(s) = - \int_0^s I_{scaled}(z) dz + Q_0$$

We also have the scaled resistance, inductance, and capacitance

$$R_{scaled} = R$$

$$L_{scaled} = L/T^*$$

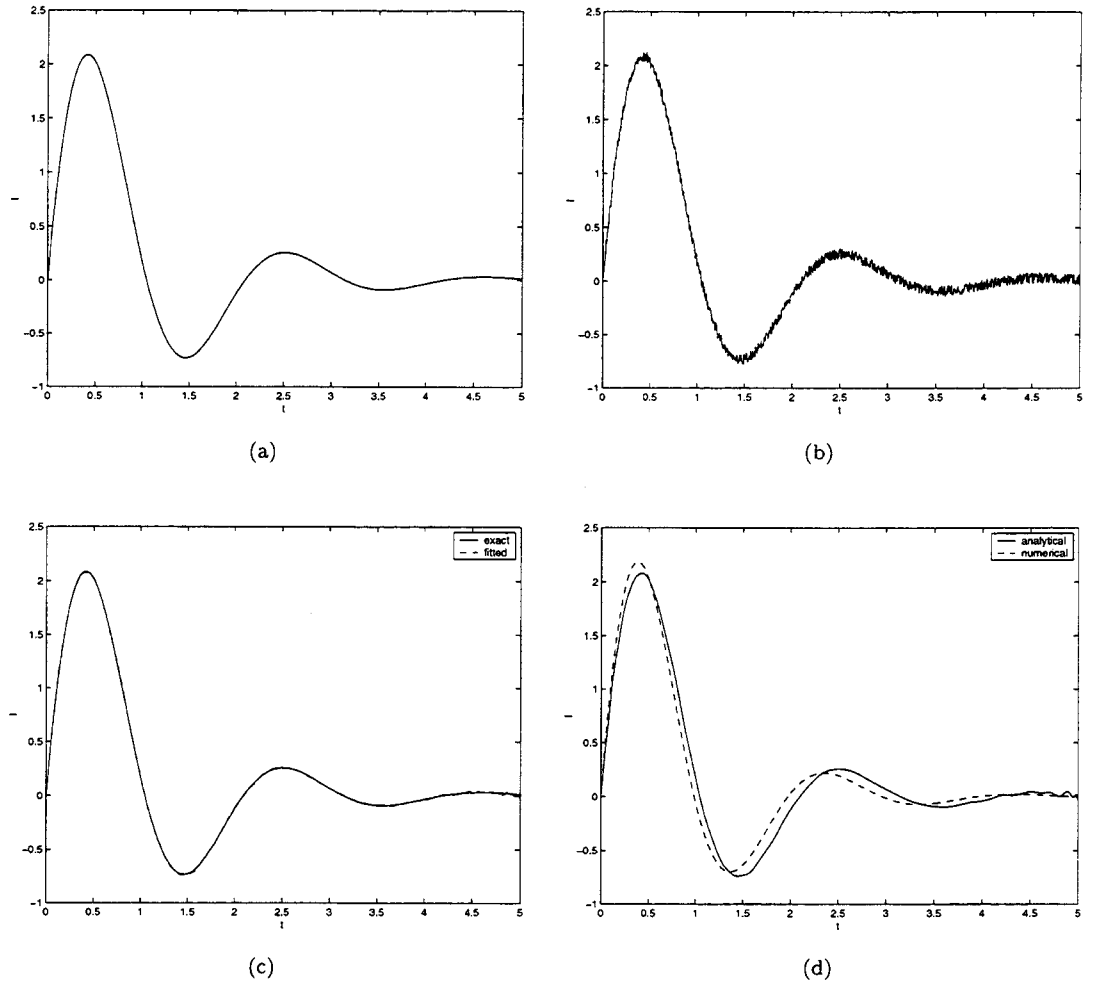


Figure 1: This is an example generated with linear circuit parameters. Figure a) shows numerically generated ring down data generated using $L = .1$, $R = .2$, and $C = 1$. Figure b) shows this same data with noise added to it (2.5 percent of the peak value). Figure c) shows our smoothed fit to the noisy data compared to the original data. Figure d) shows the output generated using the RLC values predicted by our code.

$$C_{scaled} = C/T^*$$

The equations in terms of the scaled variables can be written as

$$L_{scaled}\ddot{Q}_{scaled}(s) + R\dot{Q}_{scaled}(s) + Q(s)/C_{scaled} = 0$$

$$Q_{scaled}(0) = C_{scaled}V_0$$

In other words, the scaled system satisfies the same equations as the unscaled system, but using scaled values of time, charge, and the circuit parameters.

We have successfully gotten by without scaling our data even for circuits that discharge on the order of 10^{-5} seconds. However, if you do not scale your data, you are risking pushing the limits of whatever software you are using to solve the least squares systems. Throughout the rest of this paper we assume that we are dealing with data that has already been scaled.

The other issue of implementation we would like to address is the method for determining an analytical fit $I_{fit}(t)$ to the data, and how to obtain the derivatives and integrals of this function. We suppose that the experimental data exists from $t = 0$ to $t = T$. In order to fit the experimental data we assume that the current can be expanded in terms of Tchebychev polynomials $T_k(x)$. Tchebychev polynomials are a robust way of approximating functions on the interval $(-1, 1)$. Since we are interested in the interval $(0, T)$, we must use shifted and scaled versions of the Tchebychev polynomials. In particular, we define

$$T_k^*(t) = T_k(2t/T - 1)$$

The functions T_k^* are defined on the interval $(0, T)$, and are expressed in terms of our analytical fit to the experimental data can be written as

$$I_{fit}(t) = \sum_{k=0}^{N_{fit}} c_k T_k^*(t)$$

We determine the coefficients c_k by solving the overdetermined system of equations

$$I_{fit}(t_j) = I_e(t_j) \quad j = 1, N_{dat}$$

where t_j are the values of t where we have sampled our data, and N_{dat} is the number of data points. Assuming we have more data points than coefficients c_k , this is an overdetermined system of linear equations for the unknowns c_k . When the data is noisy, our function $I_{fit}(t)$ will also smooth the data assuming that N_{dat} is not too large.

Once we have determined the coefficients c_k , we can compute the derivatives and indefinite integrals of $I_{fit}(t)$ using simple recursions formulas derived from the properties of Tchebychev polynomials. We discuss these formulas in the appendix.

4 Nonlinear RLC Circuits

We now show how to generalize the procedure outlined in section 2) so that we can determine the functions $R(I)$, $L(I)$, and $C(Q)$ in a nonlinear RLC circuit.

As with the linear case we assume that we can smooth the data $I_e(t)$, and differentiate and integrate it to get functions $\ddot{Q}^*(t)$, $\dot{Q}^*(t)$, and $Q^*(t)$, where $Q^*(t)$ is defined in eqn. 2).

In the nonlinear case we assume that the resistances, inductances, and voltage drop across the capacitor can be written as

$$R(I) = \sum_{k=0}^{N_R-1} r_k \phi_k(I) \quad (5a)$$

$$L(I) = \sum_{k=0}^{N_L-1} l_k \phi_k(I) \quad (5b)$$

$$F(Q^*) = \sum_{k=0}^{N_C-1} f_k \psi_k(Q^*) \quad (5c)$$

Rather than defining the capacitance $C(Q)$, we are using the function $V_c(Q)$ that gives the voltage drop across the capacitor,

$$V_c(Q) = \frac{Q}{C(Q)}. \quad (6)$$

and then defining $V_c(Q)$ using the functions $F(Q^*)$.

$$V_c(Q) = F(Q - Q_0) = F(Q^*) \quad (7)$$

In eqns. 5) $\phi_k(I)$ and $\psi_k(Q^*)$ are some complete set of basis functions that allow us to approximate the nonlinear elements. For example we could choose $\phi_k(I) = I^k$. Or if we want to require that the resistance is an even function of the current we could choose $\phi_k(I) = I^{2k}$. If we want to approximate complicated functions that require large values of N_R , N_L , or N_C , it would be preferable to let the functions $\phi_k(I)$ and $\psi_k(Q^*)$ be orthogonal polynomials. However, the procedure we will now outline is the same no matter what set of basis functions ϕ_k and ψ_k we use.

We now show how to extend the analysis in the previous section to determine the coefficients r_k , l_k , and f_k , by solving an overdetermined system of linear equations.

The governing equations for a nonlinear RLC circuit are given by

$$\left(L(I) + I \frac{dL}{dI} \right) \ddot{Q} + R(I) \dot{Q} + V_c(Q) = 0$$

We also assume the initial conditions where

$$V_c(Q(0)) = V_0$$

and

$$\dot{Q}(0) = 0$$

As with the linear circuit, we introduce

$$Q^*(t) = Q(t) - Q_0$$

where Q_0 is the initial charge on the capacitor, which needs to be solved for.

In terms of the function Q^* we can write

$$\left(L(I) + I \frac{dL}{dI} \right) \ddot{Q}^*(t) + R(I) \dot{Q}^*(t) + F(Q^*) = 0$$

where

$$I = \dot{Q}^*(t)$$

$$F(Q^*) = V_c(Q^* + Q_0)$$

The condition that $V_c(Q_0) = V_0$ can be written as

$$F(0) = V_0 \quad (8)$$

If we know the coefficients $f_k, k = 1, N_C - 1$, equation 8) allows us to solve for f_0 . We want to rewrite the differential equations so they take into account the condition 8), and do not involve the coefficient f_0 . To do this we can subtract equation 8) from our governing differential equations we get the equation

$$\left(L(I) + I \frac{dL}{dI} \right) \ddot{Q}^*(t) + R(I) \dot{Q}^*(t) + F(Q^*) - F(0) = -V_0 \quad (9)$$

Assuming that $\psi_0(Q^*) = 1$, equation 9) does not involve f_0 . If we know the coefficients $f_k, k = 1, N_C - 1$ we can solve for f_0 using equation 8).

As with the linear case, we assume that we have smoothed our data and found analytical approximations to the data that give functions $Q^*(t)$, $\dot{Q}^*(t)$, and $\ddot{Q}^*(t)$. If we require that equation 9 holds at all of the data points we end up with the overdetermined system of equations

$$\ddot{Q}_j^* \left(\sum_{k=0}^{N_L-1} l_k (\phi_k(I_j) + I_j \phi'_k(I_j)) \right) + \dot{Q}_j^* \left(\sum_{k=0}^{N_R-1} r_k \phi_k(I_j) \right) + \sum_{k=1}^{N_C-1} f_k (\psi_k(Q_j^*) - \psi_k(0)) = -V_0 \text{ for } j = 1, N, \quad (10)$$

where

$$I_j = \dot{Q}(t_j)$$

$$Q_j^* = Q^*(t_j)$$

$$\dot{Q}_j^* = \dot{Q}^*(t_j)$$

$$\ddot{Q}_j^* = \ddot{Q}^*(t_j)$$

This gives us an overdetermined system of linear equations for the coefficients $r_k, k = 0, N_R - 1$; $l_k, k = 0, N_L - 1$; and $f_k, k = 1, N_C - 1$. We solve this equation in a least squares sense in order to find the coefficients r_k, l_k , and f_k . We emphasize that f_0 does not appear in these equations. Once we know f_k for $k > 0$, we solve for f_0 using

$$F(0) = V_0.$$

This now uniquely determines f_0 , and hence the function $F(Q^*)$. The function $F(Q^*)$ allows us to determine the functions $V_c(Q)$ if we know the value of Q_0 .

Assuming that we cannot use formula 3) to determine Q_0 , we will now discuss how to determine the value of Q_0 . To do this we note that when the charge is zero we have $V_c(0) = 0$, and hence

$$F(-Q_0) = 0.$$

It follows that we can find Q_0 by locating the zeros of the function $F(Q^*)$. In principle this could be done by plotting the function, and visually noting where the function crosses zero. If the function has more than one zero, then we must decide which of these to choose. The fact that the capacitance is positive implies that physical roots to $F(-Q_0) = 0$ must have $F'(-Q_0) > 0$. This eliminates some of the roots. We have never had any problems selecting the correct value of the root. If our ring down experiment is somewhat close to completely discharging the capacitor, we can choose the root that is closest to the value of Q_0 predicted by 3).

Typically we choose the basis functions $\psi_k(q^*)$ to be polynomials. In this case we can determine the roots of $F(-Q_0)$ by finding the roots of polynomials. Typically this is done by finding the eigenvalues of the companion matrix associated with that polynomial. In general this procedure will give multiple roots that we need to choose from. We select these roots as described in the last paragraph. Once we have determined Q_0 , we use equation 7) to determine the voltage drop $V_c(Q)$ across the capacitor. We then determine the capacitance $C(Q)$ using

$$C(Q) = \frac{Q}{V_c(Q)}.$$

We now briefly outline the algorithm for determining the functions $R(I)$, $L(I)$, and $C(Q)$ in a nonlinear RLC circuit. We describe the algorithm assuming that we have already scaled our data as described in section 3).

- Find a curve fit $I_{fit}(t)$ that approximates the experimental data $I_e(t)$.
- Integrate and differentiate this data to get the function $Q^*(t)$ and its first two derivatives.

- Choose a set of basis functions $\phi_k(I)$ to approximate the resistances and inductances. Also choose a set $\psi_k(Q^*)$ to approximate the function $F(Q^*)$.
- Choose the number of functions N_R , N_L , and N_C that we will use to approximate $R(I)$, $L(I)$, and $F(Q^*)$.
- Solve the overdetermined set of equations 10) to determine the parameters $r_k, k = 1, N_R - 1$; $l_k, k = 0, N_L - 1$; and $f_k, k = 1, N_C - 1$.
- Use the equation 8) to determine the parameter f_0 .
- Solve the equation $F(-Q_0) = 0$ to determine the value of Q_0 , and hence determine the function $V_c(Q)$ using 7) .
- Solve for $C(Q)$ using 6).

5 Some Non-linear Examples from Numerically Generated Data

It is risky to draw general conclusions from a small number of examples. Never the less, we will present a few examples that illustrate the performance of this algorithm on some test problems.

5.1 Non-linear L

In this example we keep R and C constant, but let L vary. In particular we set $R = .2$, $C = 1.$, and

$$L(I) = .1e^{I^2}$$

We use the initial condition $Q(0) = 1$, and integrate these equations from $t = 0$ to $t = 5$.

In the examples that we give we have generated data by solving the governing differential equations numerically with these values of R , L and C .

Figures 2a) shows the predicted function $L(I)$ that we get when we use our algorithm assuming that $L(I)$ is a linear function of I^2 . Figure 2b) shows the current produced by our function $L(I)$ compared to the true current. Figure 3) shows the same example but where we have used a quadratic function of I^2 for $L(I)$. If we use higher order polynomials to approximate $L(I)$ we get even better results.

We now add some random noise to our numerically generated data. Figure 4a) shows the noisy data, and figure 4b) shows how our fit to this noisy data agrees with the exact solution. Once again we note that true ring down data might not have this high frequency noise that we have used, but the fitted data has gotten rid of this high frequency noise, and replace it with low frequency noise. Figure 5) shows the predicted values of $L(I)$ and $I(T)$ using our algorithm

(with $L(I)$ a quadratic function of I^2) on the fit to the noisy data. Figure 6) shows our algorithm on this same data but where we have assumed that $L(I)$ is a fifth order polynomial in I^2 . This does not give any better results than when we assumed a quadratic polynomial, but it is encouraging that we do not get worse results either.

On this particular problem the algorithm seems to give quite reasonable results even in the presence of noise.

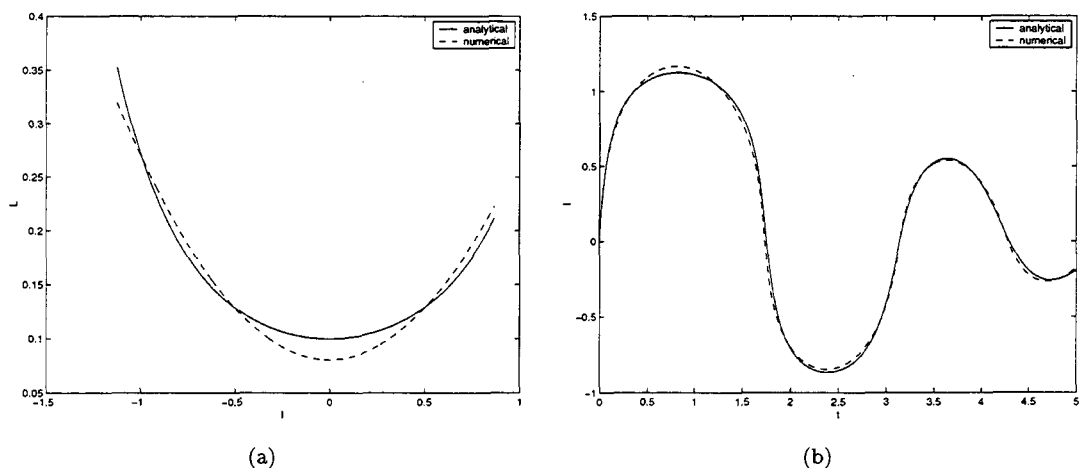
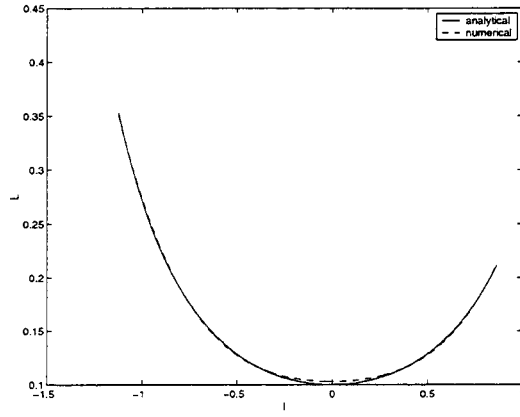


Figure 2: This is an example with $L(I) = .1e^{I^2}$, $R = .2$, and $C = 1$. We are fitting the data with R and C constant, and with L a linear function of I^2 . a) The agreement between the exact function $L(I)$ and the fitted function $L_{fit}(I)$. b) The agreement between the exact current $I(t)$, and the current generated by the fitted function $L_{fit}(I)$.

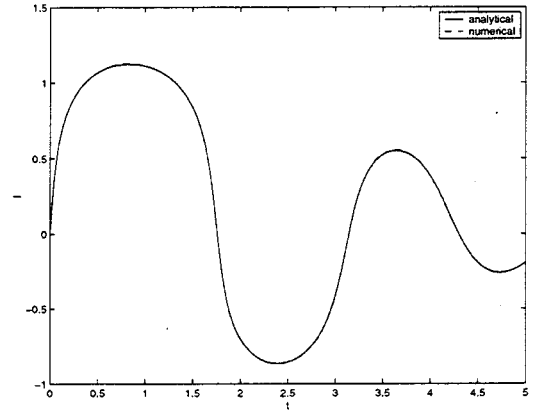
5.2 Trying to Fit a Current Distribution Not Produced by an RLC Circuit

We now ask the question; is it possible to find functions $L(I)$, $R(I)$, and $C(Q)$ that fit any current distribution $I(t)$ that we specify; even if $I(t)$ was not generated by an RLC circuit? It appears that this might be possible since we have infinitely many degrees of freedom in specifying these functions. We will now give an example that shows that it is not possible to fit totally arbitrary functions $I(t)$.

In this example we will assume that we are given R and C as positive

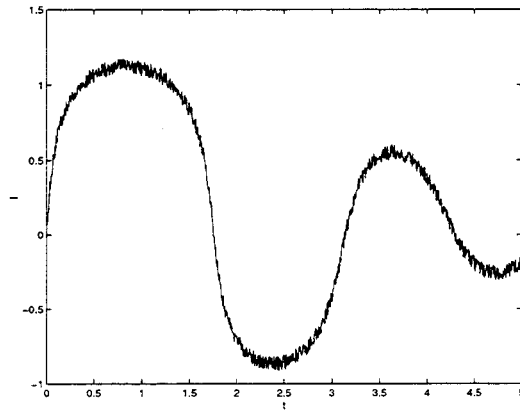


(a)

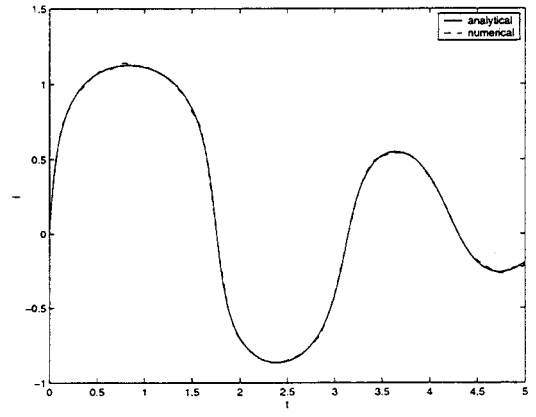


(b)

Figure 3: This is the same example as in figure 1) except we have used a quadratic polynomial in I^2 to fit $L(I)$.



(a)



(b)

Figure 4: a) The exact current data for figure 1) with random noise added. b) The fit to the noisy data compared to the exact data.

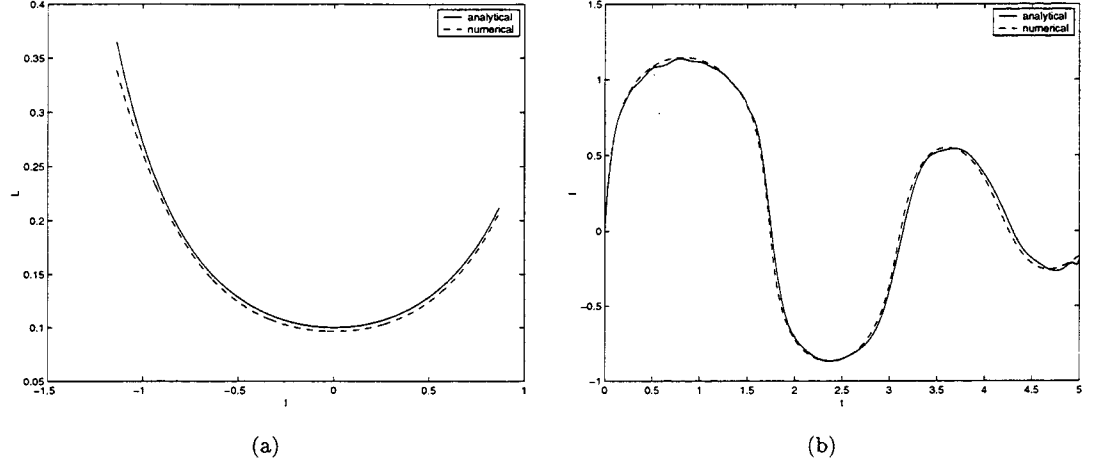


Figure 5: This is the same example as in figures 1) and 2) except we have added noise to the current before we fit it. We are using a quadratic polynomial in L to fit the data.

constants, and that we are trying to find a function $L(I)$ that will fit the ring down data $I(t) = t^2 - t^3$. This is not precisely the problem we have been talking about, since R and C are specified, but we could modify our procedure to handle this situation. We will prove that it is impossible to find a function $L(I)$ that fits this data. This shows that the argument that we can fit any data because we have infinitely many degrees of freedom is not correct. We will then present numerical evidence that shows that we cannot fit this current distribution even when we let R and C vary.

We begin by defining the function

$$G(I) = L(I) + I \frac{dL}{dI}$$

Our governing differential equation can be written as

$$G(I)\ddot{Q} + R\dot{Q} + Q/C = 0$$

If we could find a function $G(I)$ that fit the data $t^2 - t^3$, then evaluating the equation at $t = 0$ shows that $G(0) > 0$, and $Q(0) = 0$. Taking the derivative of our differential equation and evaluating the result at $t = 0$, we see that

$$G(0)\ddot{I} + G'(0)\dot{I}^2 + R\dot{I} = 0$$

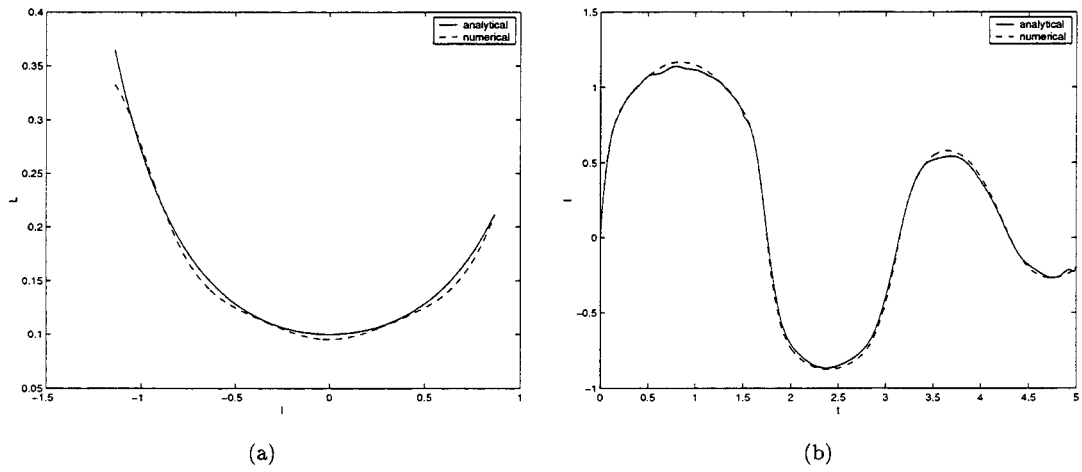


Figure 6: This is the same example as in figure 4) except we have used a fifth order polynomial in I^2 to fit $L(I)$. Due to the noise we have added onto the data, the results are no better than in figure 4). However, it is encouraging that the results are not worse either.

Since $\ddot{I}(I) > 0$, we see that we must have

$$G'(0) < 0$$

We now consider the situation at $t = 1$. We have $I(1) = 0$, and $\dot{I}(1) < 0$, and $\ddot{I}(1) < 0$. If we once again take the derivative of the governing differential equation and evaluate it at $t = 1$, we get

$$G(0)\ddot{I}(1) = -R\dot{I}(1) - G'(0)\dot{I}(1)^2$$

Since we know that $G'(0) < 0$, this implies that we must have $\ddot{I}(1) > 0$. However, this contradicts the fact that the function $t^2 - t^3$ has a negative second derivative at $t = 1$. It follows that it is not possible to find any function $G(I)$ that fits this current distribution.

Figure 7) shows an attempt to fit this current distribution where we assume that R and C are unspecified constants, and that L is an arbitrary function. No matter how many terms we take in our expansion of $L(I)$, we do not get any improvement in our results. Similar results hold even when we let R and C be more complicated functions.

5.3 Non-Linear R

We now give an example where the inductance and capacitance are constant, but the function $R(I)$ depends on I . In particular, we choose $L = .1$, $C = 1.$, and

$$R(I) = .2/(1 + I^2/2)$$

Once again we generate our data by numerically integrating the governing differential equations on the interval from $t = 0$ to $t = 5$.

Figures 8) , and 9) and 10) show the performance of our algorithm when there is no noise present. We are fitting L and C assuming that they are constants, and we use linear, quadratic, and quintic polynomials in I^2 for the function $R(I)$. We get progressively better agreement as we approximate $R(I)$ with more powers of I^2 . When we use a quintic polynomial in I^2 we are getting nearly perfect agreement both with our prediction for the function $R(I)$, and with our prediction of the current (using our predicted value of $R(I)$).

In order to test the algorithm with noise present we have added ten percent random noise to the data. Figure 11a) shows the noisy data, and figure 11b) shows the fit to the noisy data compared to the exact data. Figures 12) and 13) show the performance of our algorithm when we try to fit the smoothed data. The functions $R(I)$ that we obtain in this way are in fairly good agreement with the true values of $R(I)$, but they clearly have some features that are artifacts.

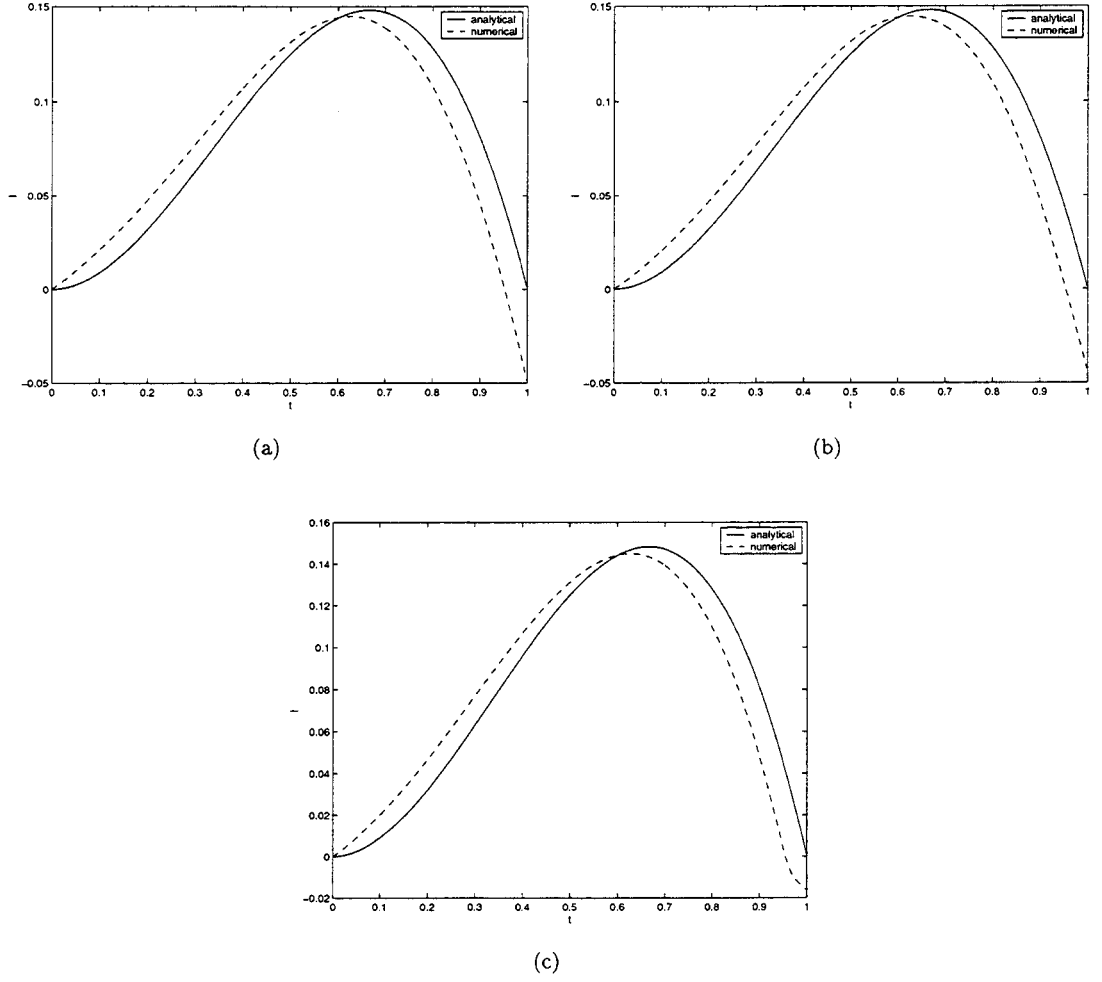


Figure 7: This shows an attempt to fit a current distribution that was not derived from the output of an RLC circuit. The current is $I(t) = t^2 - t^3$. We are trying to fit this function using a nonlinear L , and constant values for R and C . No matter how many terms in our expansion for $L(I)$ we choose, we cannot find a function $L(I)$ that fits the current distribution . a) Using a constant value of L . b) using a quadratic function of I^2 . c) Using a tenth order polynomial in I^2 for $L(I)$.

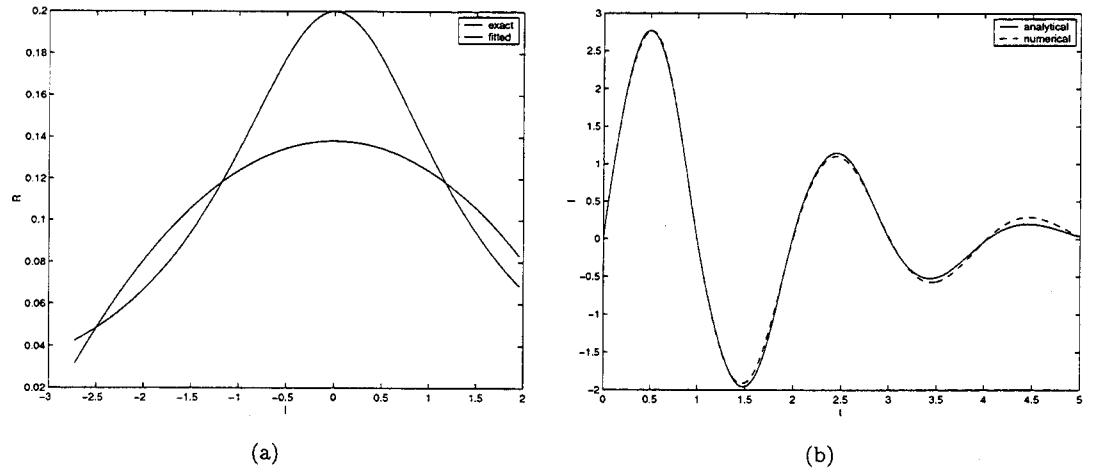
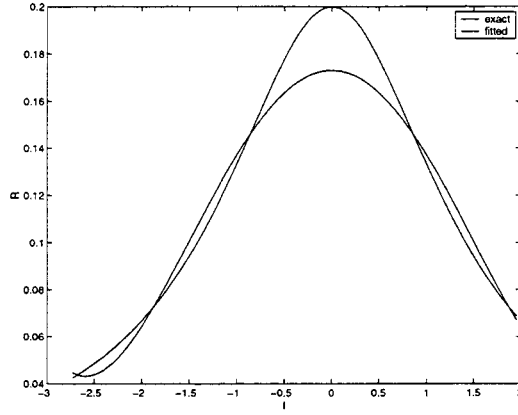
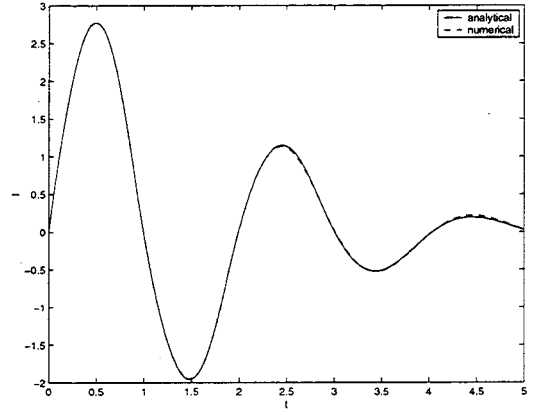


Figure 8: This is an example with $L = .1$, $C = 1.$, and $R = .2/(1+I^2/2)$. We are fitting the data with L and C constant, and with R a linear function of I^2 . a) The agreement between the exact function $L(I)$ and the fitted function $L_{fit}(I)$. b) The agreement between the exact current $I(t)$, and the current generated by the fitted function $L_{fit}(I)$.

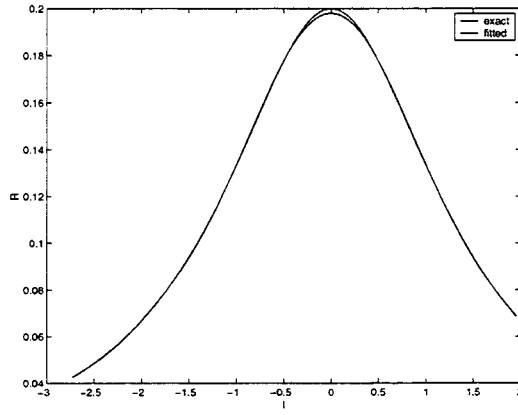


(a)

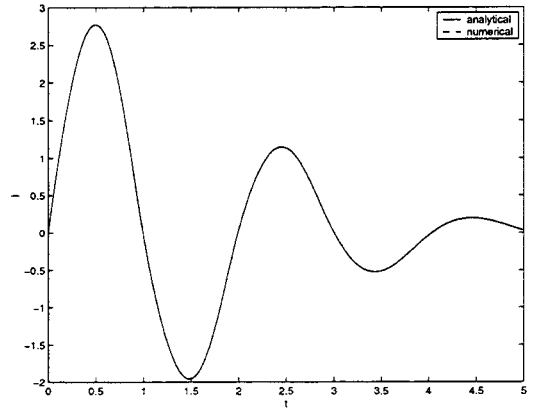


(b)

Figure 9: This is the same example as in figure 8) except we have used a quadratic polynomial in I^2 to fit $R(I)$.



(a)



(b)

Figure 10: This is the same example as in figure 8) except we have used a quintic polynomial in I^2 to fit $R(I)$.

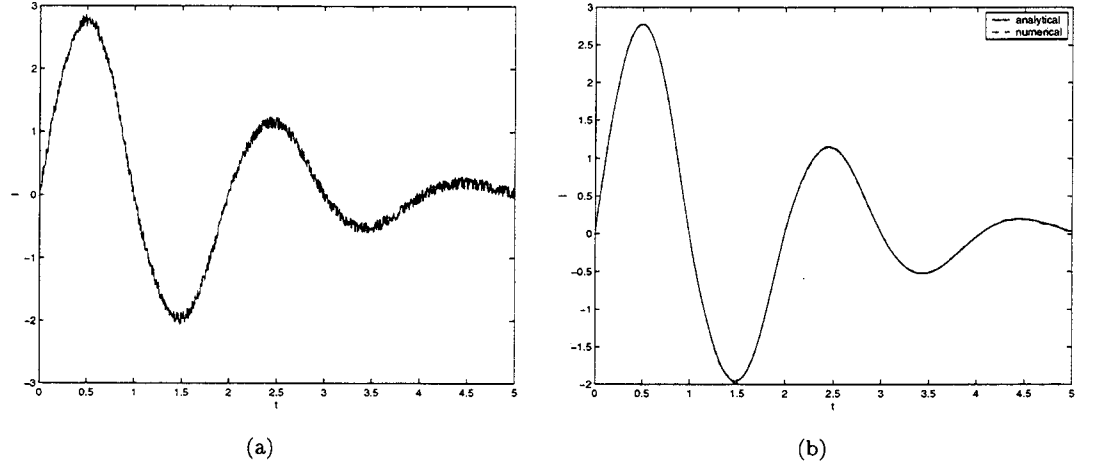


Figure 11: a) The exact current data for figure 8) with random noise added. b) The fit to the noisy data compared to the exact data.

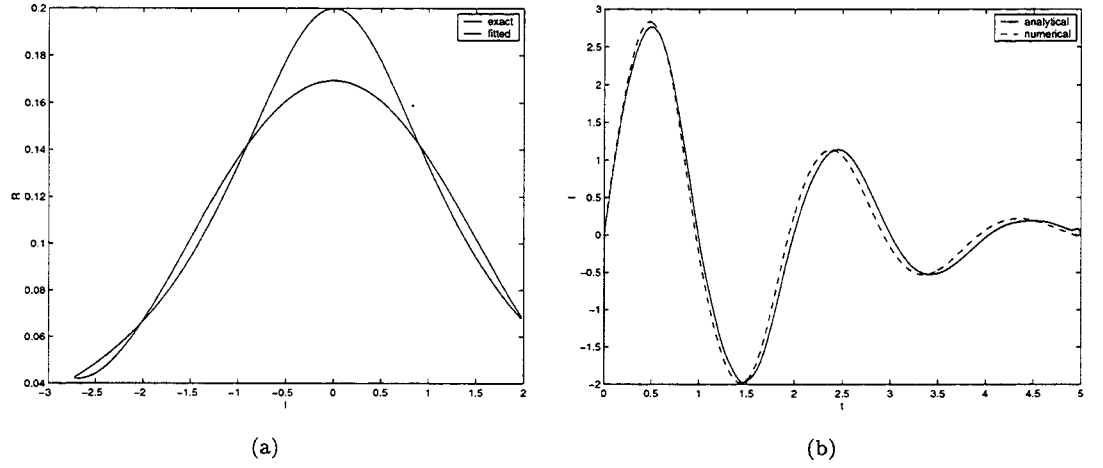


Figure 12: This is the same example as in figures 8) ,9) and 10) except we have added noise to the current before we fit it. We are using a quadratic polynomial in R to fit the data.

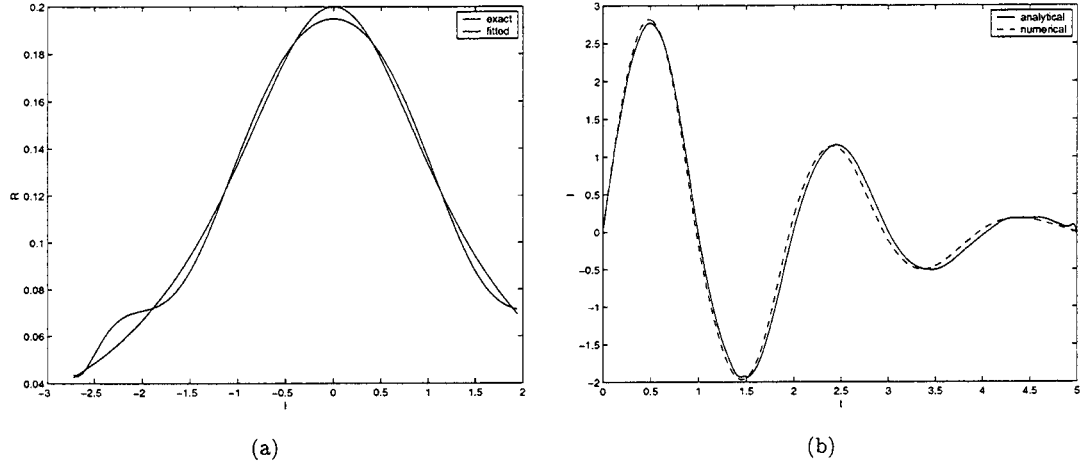


Figure 13: This is the same example as in figure 12) except we have used a fifth order polynomial in I^2 to fit $R(I)$.

5.4 Non-Linear C

We now give an example where we have R and L constant, but have C vary with Q . In particular, we set $L = .1$, $R = .2$, and

$$C(Q) = \exp(-Q^2/2)$$

We generate the data by numerically integrating the governing differential equations with the initial condition $Q(0) = 1$, and $\dot{Q}(0) = 0$. We give the data on the interval $t = 0$ to $t = 5$.

Note that eventhough C is an even function of Q , our algorithm does not allow us to take this symmetry into account.

Figures 14) and 15) show how our algorithm works without any noise present. We assume that R and L are constants, and we fit $F(Q^*)$ using a cubic and a quintic polynomial. The cubic polynomial already gives quite good results, and the quntic polynomial gives excellent agreement both for the function $C(Q)$, and for the current distribution predicted by this function.

We now consider the algorithm with some noise present. Figure 16a) shows the result of adding 10 percent random noise to the exact current distribution. Figure 16b) shows our smoothed fit to the noisy data, and how it compares to the exact current distribution. Figures 17) and 18) show the performance of our algorithm on this smoothed data. Here we are using cubic and quintic approximations to the function $F(Q^*)$. The noise has added some significant

distortion to the profile for $C(Q)$. In figures 17c) and 18c) we show how the voltage drop $Q/C(Q)$ across the capacitor compares to the exact value. We see that we have done a better job of fitting this function. However, our predicted value of the current also seems to be more sensitive to the noise than it was in the cases when L and R were nonlinear.

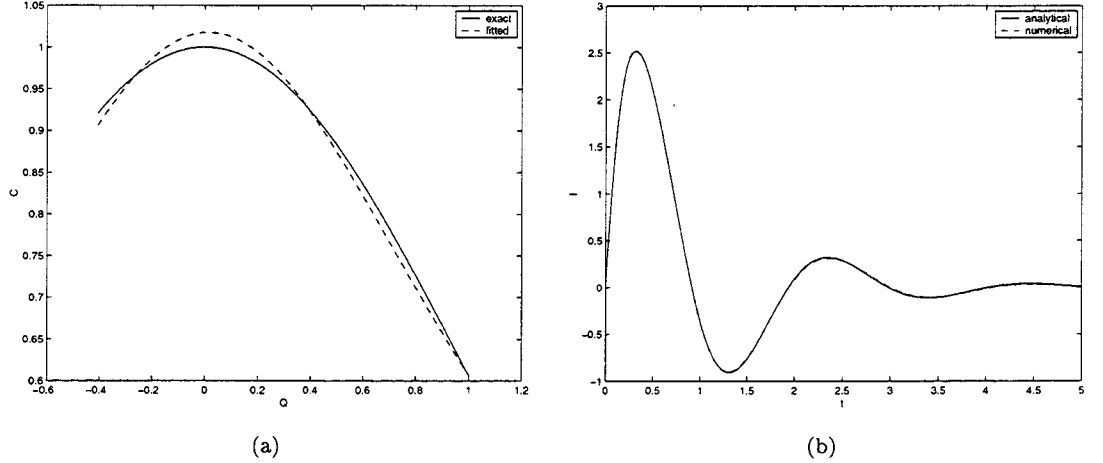


Figure 14: This is an example with $C(Q) = e^{-Q^2/2}$, $R = .2$, and $L = .1$. We are fitting the data with R and L constant, and with $F(Q^*)$ a cubic function of Q^* . a) The agreement between the exact function $C(Q)$ and the fitted function $C_{fit}(Q)$. b) The agreement between the exact current $I(t)$, and the current generated by the fitted function $C_{fit}(Q)$.

6 Examples Using Real Data

We will now give some examples of the performance of the algorithm on some real experimental data. All of our examples are from a single circuit that was initially charged up to different voltages.

6.1 Experimental Data -200 Volts

We now consider the performance of the algorithm on some experimental data. This particular set of data was believed to be fairly close to a linear regime of the circuit elements. Figure 19) shows the current distribution from some

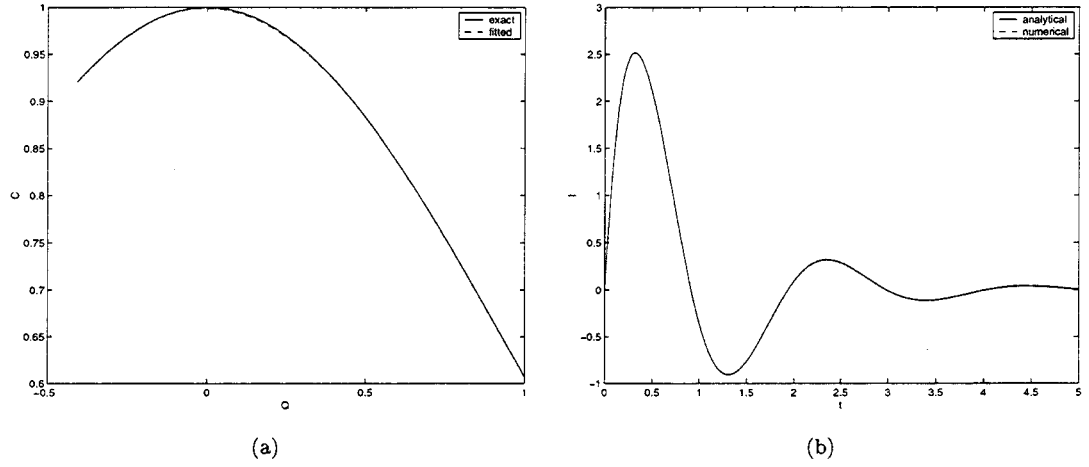


Figure 15: This is the same example as in figure 14) except we have used a quintic polynomial in Q to fit $F(Q^*)$.

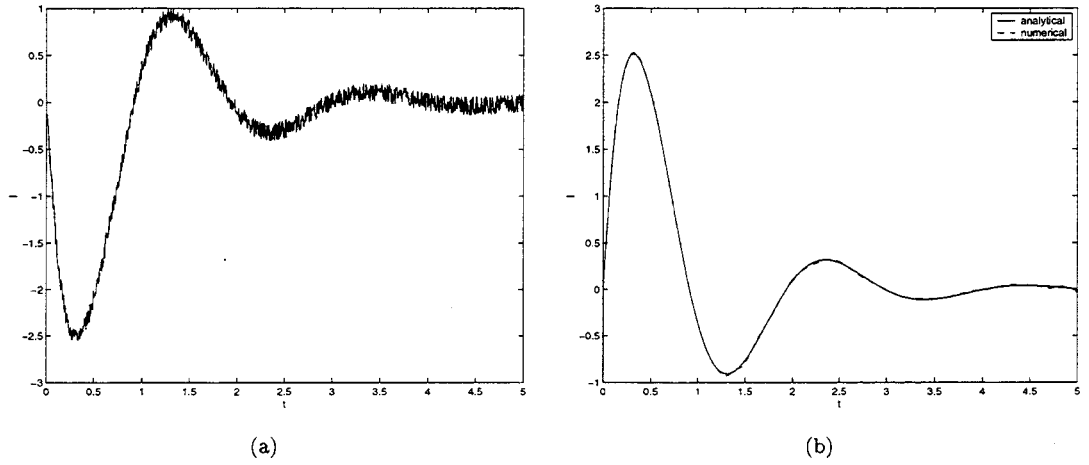


Figure 16: a) The exact current data for figure 14) with random noise added.
b) The fit to the noisy data compared to the exact data.

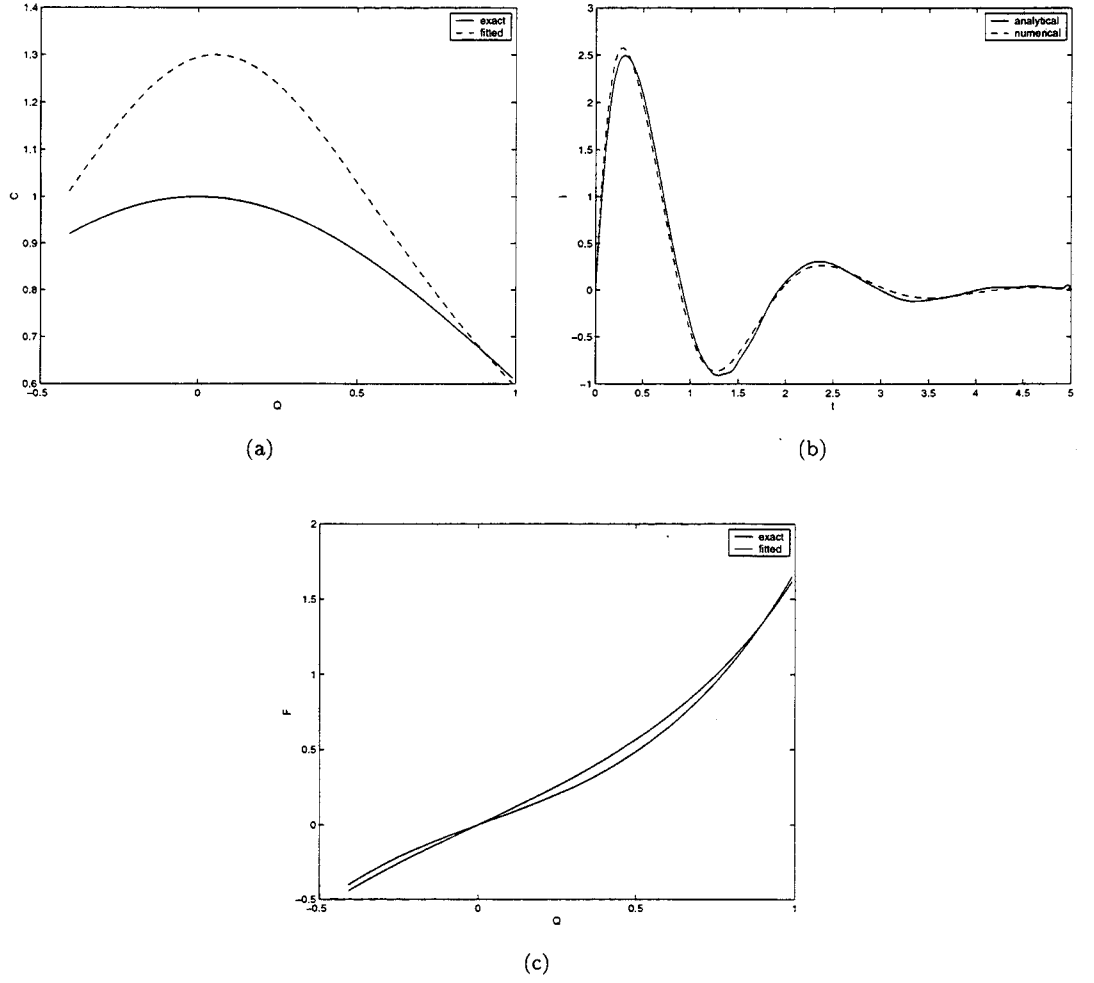
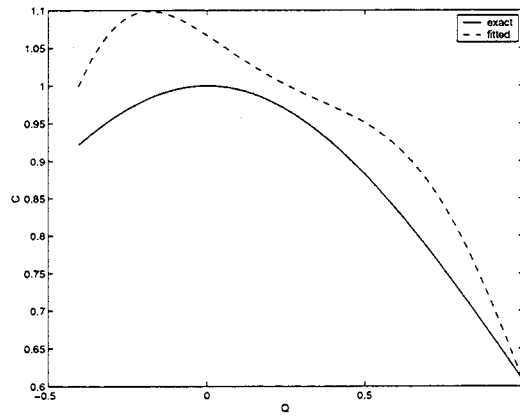
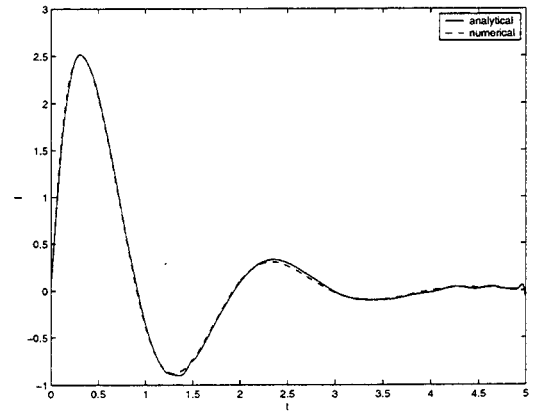


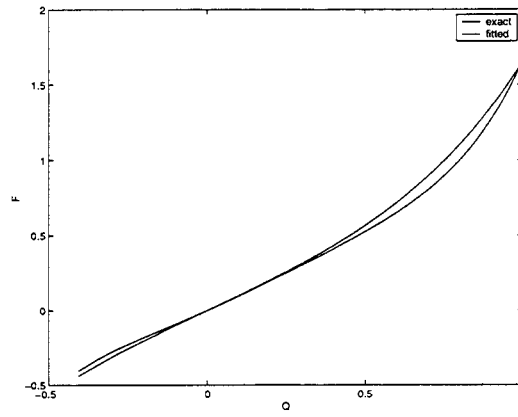
Figure 17: This is the same example as in figures 14) and 15) except we have added noise to the current before we fit it. We are using a cubic polynomial in $F(Q^*)$ to fit the data.



(a)



(b)



(c)

Figure 18: This is the same example as in figure 4) except we have used a quintic polynomial in Q^* to fit $F(Q^*)$.

real ring down data. We see that the data has a considerable amount of high frequency noise on it. Figure 19) also shows the smoothed approximation to the data.

We begin by trying to fit this data assuming that R , L and C are all constant. Figure 20a) shows the current distribution predicted by the values of R , L and C coming out of our algorithm. The fit to the experimental data is not bad. Figure 20b) shows the curve fit to the experimental data that we get by assuming that R and L are linear functions of I^2 , and that F is a cubic function of Q^* . This gives us excellent agreement with the experimental data. Including higher order nonlinearities does not improve the fit to the data.

Figure 21) shows the functions L , R and C obtained using our algorithm.

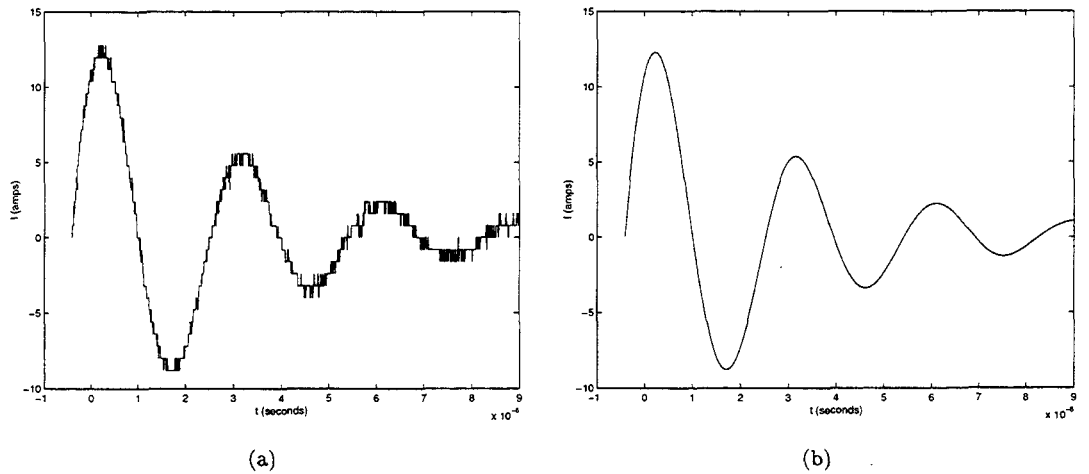


Figure 19: This is an experimentally measured current distribution. We have multiplied the time by 10^5 in order to better scale our equations. a) The original data. b) The smoothed data.

6.2 Experimental Data - 500 Volts

This set of experimental data uses the same circuit elements as in the last example, but is initially charged up to a higher voltage. Figure 22a) shows the noisy experimental data, and figure 22b) shows the smoothed fit to this data. Figure 23a) shows the current distribution obtained by assuming that all of the circuits parameters R , L and C are constant. We see that we are not getting as good a fit as we did in the last example because the circuit is in a regime where

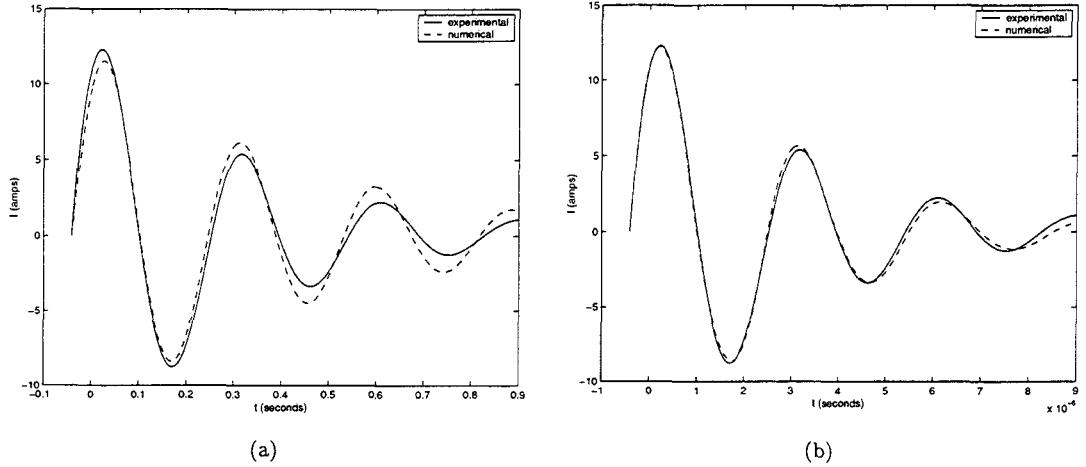


Figure 20: This shows the numerically predicted current compared to the smoothed experimentally determined current. a) R , L and C assumed constant. b) R and L linear in I^2 , F a cubic in Q^* .

nonlinearities are more important. Figure 23b) shows the fit to the current distribution obtained by assuming that R and L are linear functions of I^2 and that $F(Q^*)$ is a cubic function of Q^* .

6.3 Experimental Data- 1000 Volts

This is the same as the previous two examples but the capacitor is initially charged to 1000 volts. Figure 25) shows the noisy data and our smoothed fit to it. Figure 26a) shows The fit to the data current when we assume constant values for R , L and C . Figure 26b) shows the fit to the current when we use linear functions of I^2 for R and L , and a quintic function for $F(Q^*)$. Figure 27) shows our prediction of the functions R , L , and C .

6.4 Comparison of Different Experimental Shots

The last three examples were all created using the same circuit. Each set of experiments determines the functions $R(i)$, $L(I)$, and $C(Q)$ on different intervals. The higher the voltage is, the larger the interval is. We now compare the circuit parameters predicted by the three different experiments on the intervals determined by the data taken for the 200 Volt ring down. In figures 29),

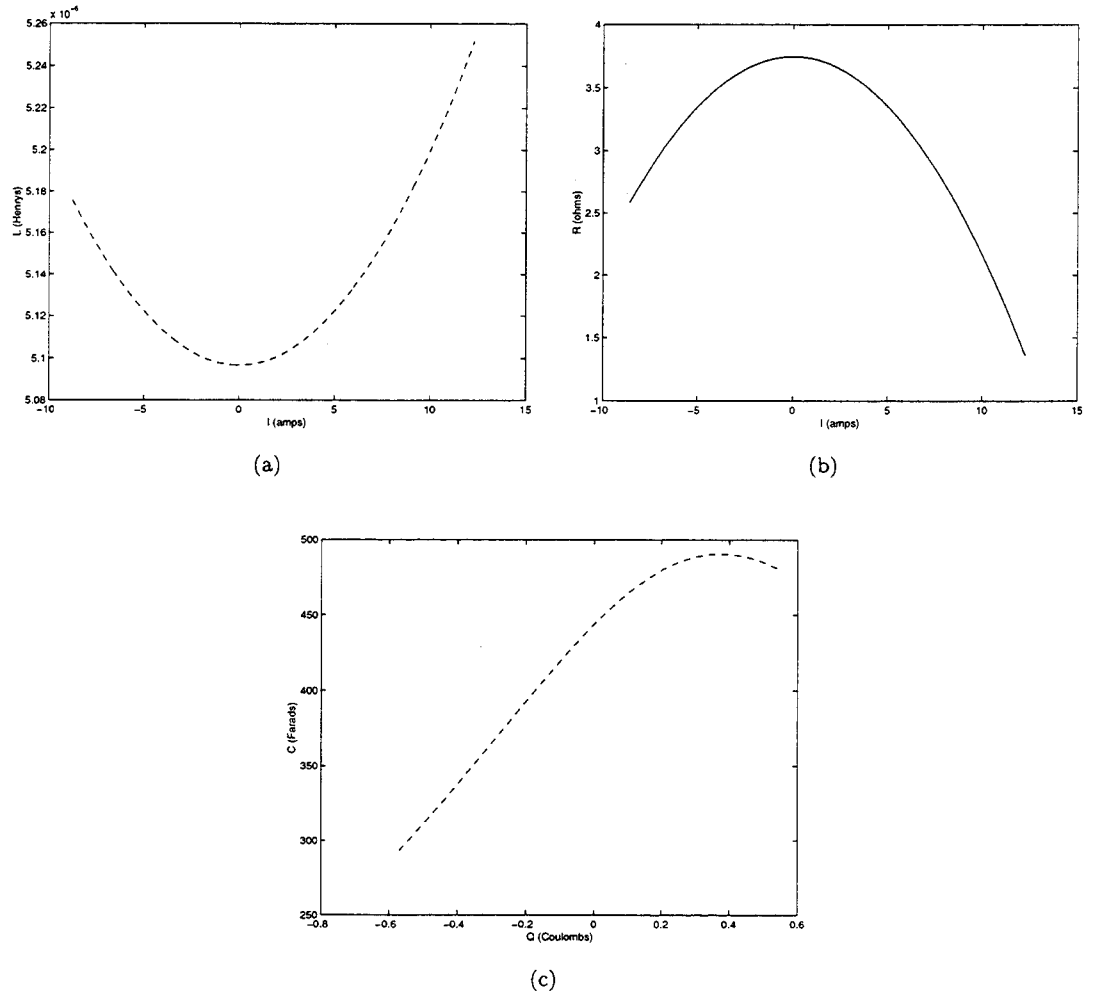


Figure 21: The predicted values of the resistance $R(I)$, the inductance $L(I)$, and the capacitance $C(Q)$ for the experimentally determined current in figure 19).

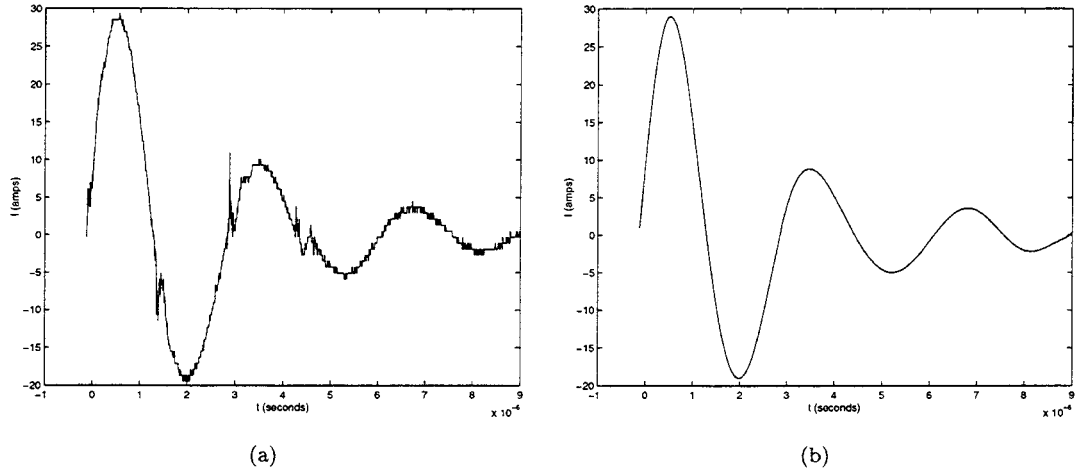


Figure 22: This is an experimentally measured current distribution. We have multiplied the time by 10^5 in order to better scale our equations. a) The original data. b) The smoothed data.

29), and 30) we show the functions $C(Q)$, $R(I)$, and $L(I)$ predicted by each individual ring down experiment. We see that the results from each experiment predict functions that are not in exact agreement with each other, but that are relatively close to each other.

Acknowledgments We would like to acknowledge Lou Weichman for motivating this problem and supporting the work, Ginger de Marquis for supplying the experimental data, and Stephen Yao for assisting with the figures..

References

- [1] W.J. Cunningham. *Introduction to Nonlinear Analysis*. McGraw Hill (New York), 1958.
- [2] F. Kouril and K. Vrba. *Non-Linear and Parametric Circuits: Principles, Theory, and Applications*. Halsted (Chichester), 1988.
- [3] M.E. van Valkenburg. *Network Analysis*. Prentice Hall (New Jersey), 1974.

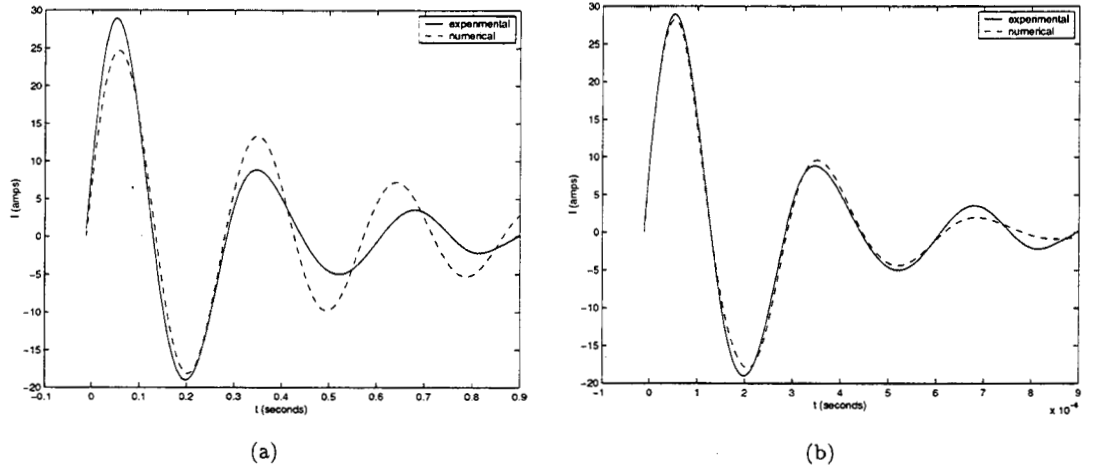


Figure 23: This shows the numerically predicted current compared to the smoothed experimentally determined current. a) R , L and C assumed constant. b) R and L linear in I^2 , F a cubic in Q^* .

7 Appendix

In this appendix we give some of the necessary formulas involving Tchebychev polynomials. We suppose we have a function $f(t)$ that is represented in terms of shifted Tchebychev polynomials $T_k^*(t) = T_k(2t/T - 1)$.

$$f(t) = \sum_{k=0}^N c_k T_k^*(t)$$

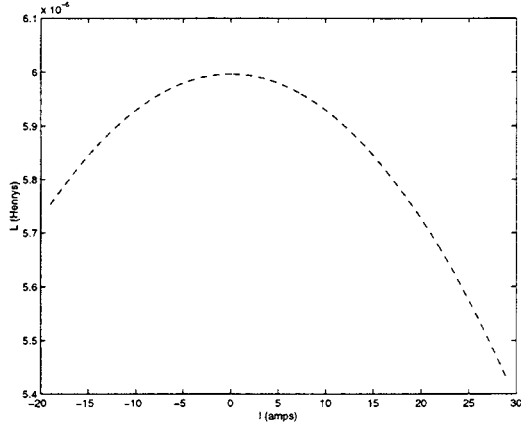
We would like to express the the derivative and integral in terms of the functions T_k^* . In particular we write

$$\frac{df}{dt} = \sum_{k=0}^N c'_k T_k^*(t)$$

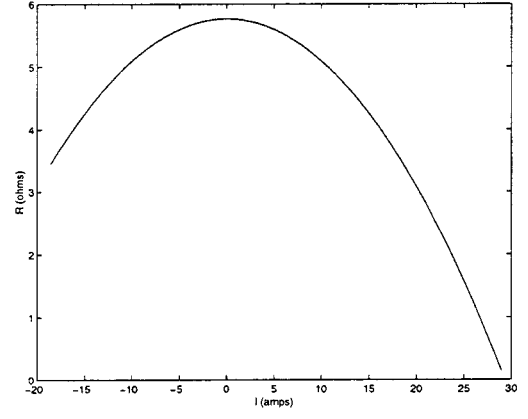
$$\int_0^t f(s) ds = \sum_{k=0}^N C_k T_k^*(t)$$

The coefficients c'_k are given by

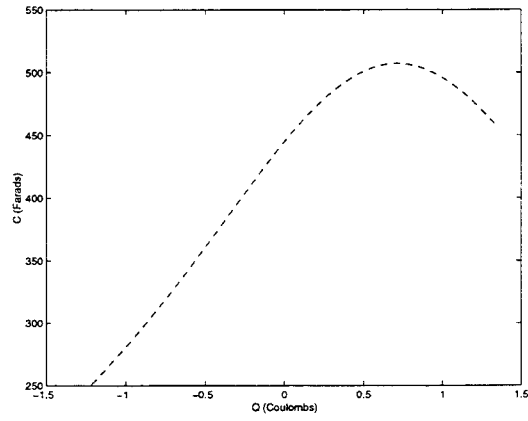
$c'_k = 0$ for all $k \geq N$. The remaining coefficients are given by:



(a)



(b)



(c)

Figure 24: The predicted values of the resistance $R(I)$, the inductance $L(I)$, and the capacitance $C(Q)$ for the experimentally determined current in figure 22).

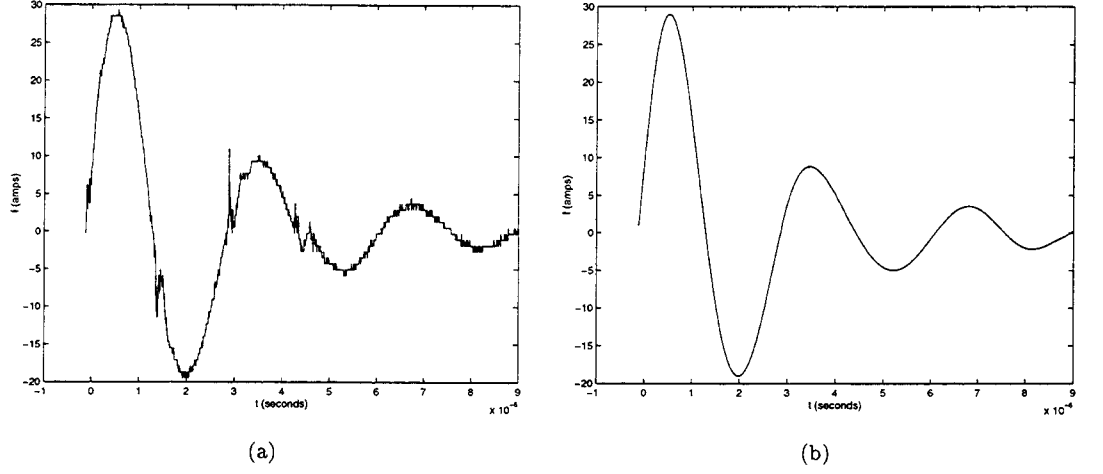


Figure 25: This is an experimentally measured current distribution. We have multiplied the time by 10^5 in order to better scale our equations. a) The original data. b) The smoothed data.

$$a_k c'_k = c'_{k+2} + \frac{2}{T} 2(k+1) c_{k+1}, \quad 0 \leq k \leq N-1, \quad (11)$$

where

$$a_k = \begin{cases} 2 & \text{if } k = 0, \\ 1 & \text{if } k \geq 1. \end{cases}$$

The coefficients C_k are given by

$$C_k = \frac{T}{2} \left(\frac{c_{k-1} - c_{k+1}}{2(k-1)} \right), \quad 2 < k < N \quad (12)$$

$$C_{N+1} = \frac{T}{2} \frac{c_N}{2N}$$

and

$$C_N = \frac{T}{2} \frac{c_{N-1}}{2(N-1)}.$$

$$C_1 = \frac{T}{2} \left(c_0 - \frac{c_2}{2} \right).$$

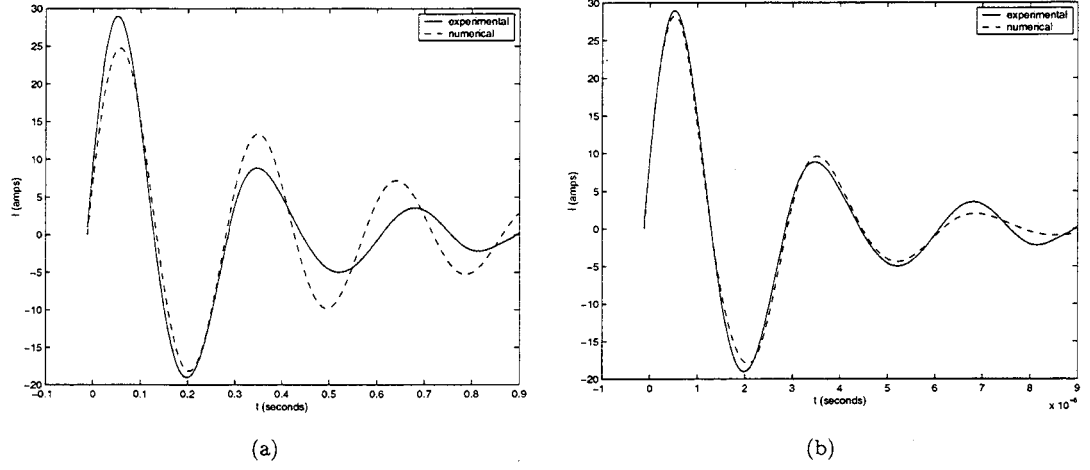
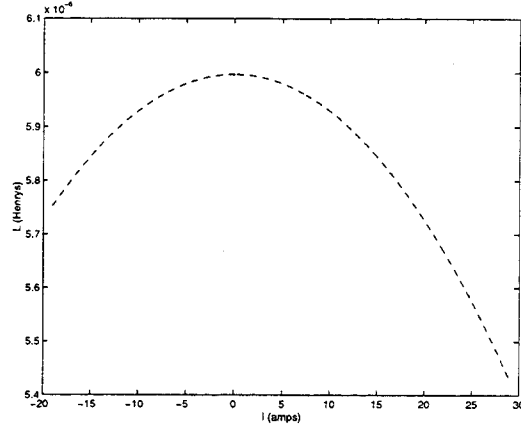


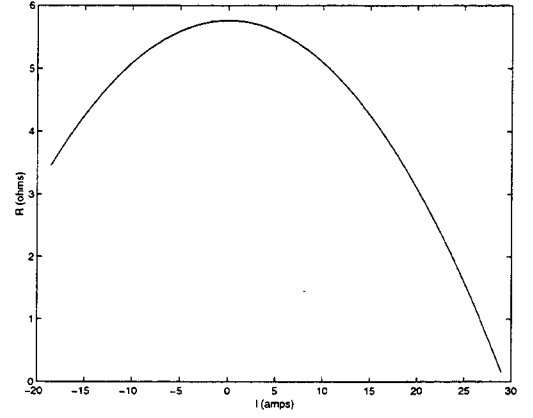
Figure 26: This shows the numerically predicted current compared to the smoothed experimentally determined current. a) R , L and C assumed constant. b) R and L linear in I^2 , F a cubic in Q^* .

This gives us our final special case:

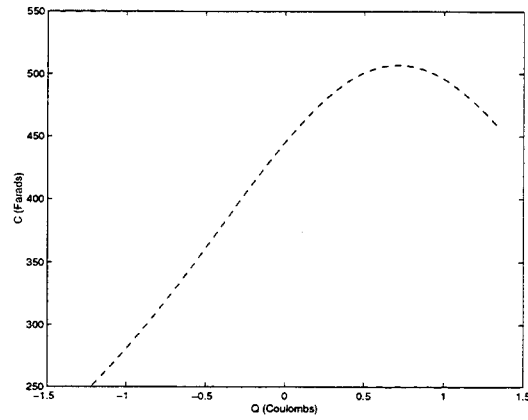
$$C_0 = \sum_{k=1}^{N+1} (-1)^{k-1} C_k$$



(a)

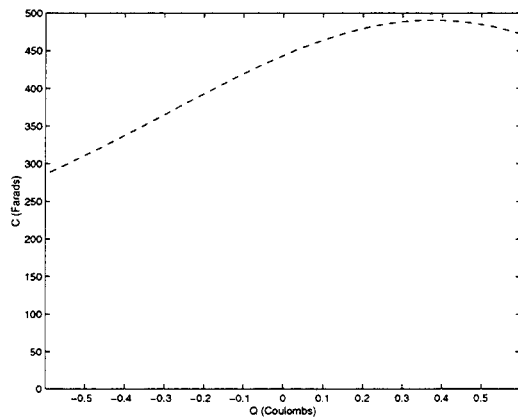


(b)

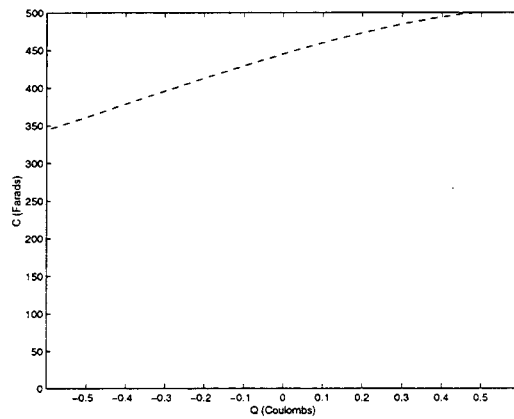


(c)

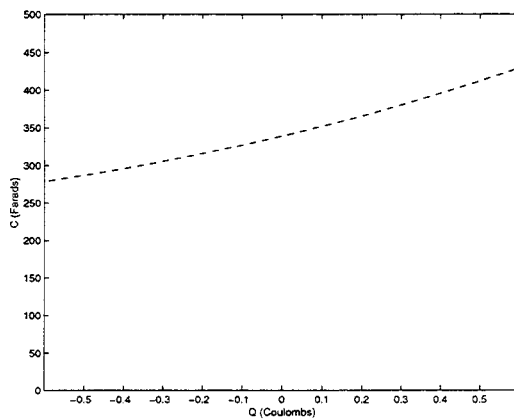
Figure 27: The predicted values of the resistance $R(I)$, the inductance $L(I)$, and the capacitance $C(Q)$ for the experimentally determined current in figure 25).



(a)

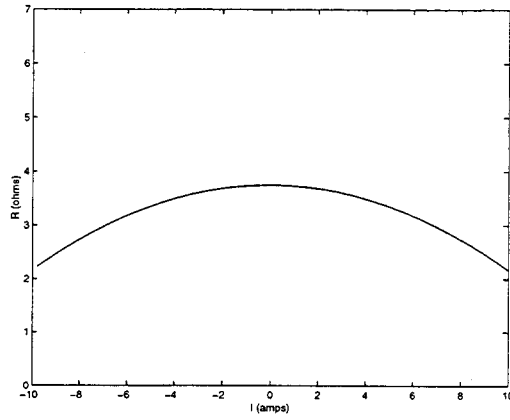


(b)

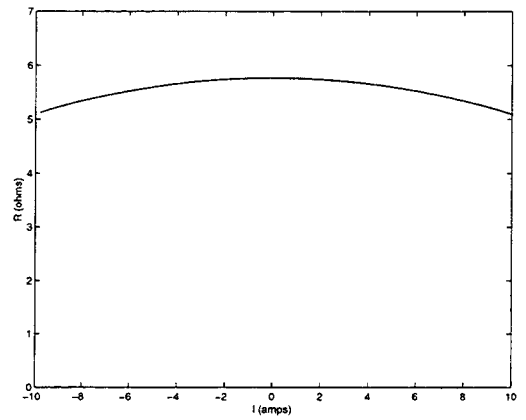


(c)

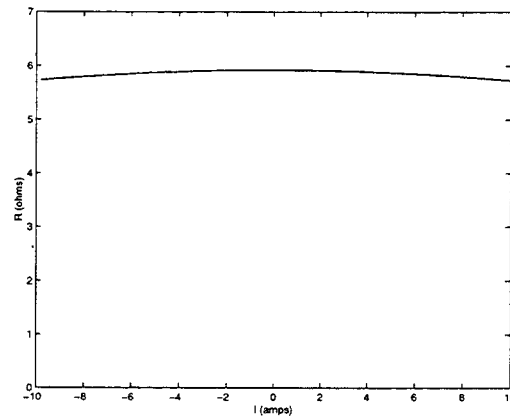
Figure 28: This shows the function $C(Q)$ predicted by the three different sets of ring down experiments. We only show the functions on the interval Q for the data obtained with 200V. a) 200 Volts b) 500 Volts c) 1000 Volts.



(a)

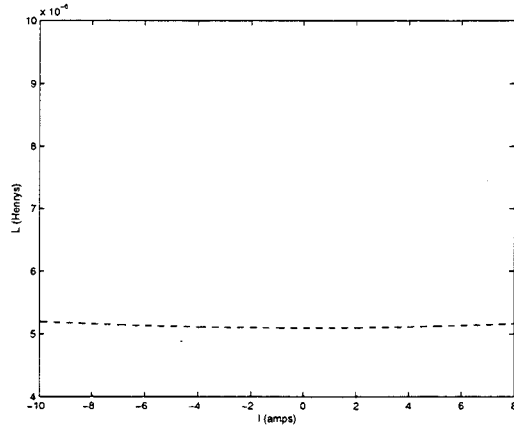


(b)

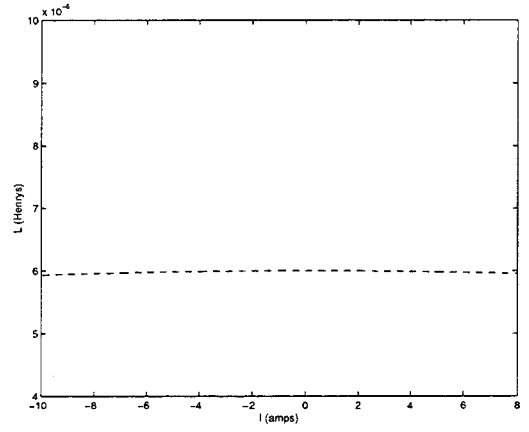


(c)

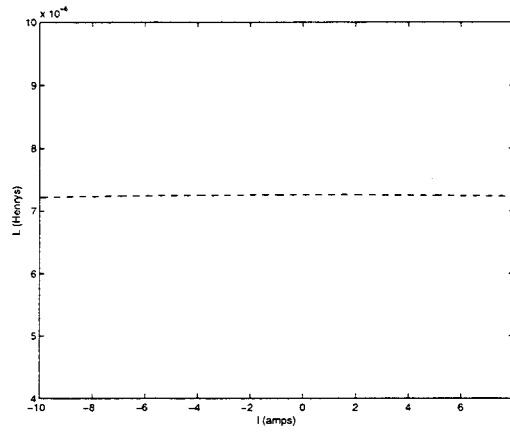
Figure 29: This shows the function $R(I)$ predicted by the three different sets of ring down experiments. We only show the functions on the interval Q for the data obtained with 200V. a) 200 Volts b) 500 Volts c) 1000 Volts.



(a)



(b)



(c)

Figure 30: This shows the function $R(I)$ predicted by the three different sets of ring down experiments. We only show the functions on the interval Q for the data obtained with 200V. a) 200 Volts b) 500 Volts c) 1000 Volts.

DISTRIBUTION

| | | | |
|---|----------|--------------------------------|-------|
| 1 | MS 1423 | P. A. Miller | 1118 |
| 1 | MS 0529 | B. C. Walker | 2600 |
| 1 | MS 0319 | L. D. Hostetler | 2610 |
| 1 | MS 0328 | J. A. Wilder Jr. | 2612 |
| 1 | MS 0328 | F. M. Dickey | 2612 |
| 1 | MS 0328 | S. E. Yao | 2612 |
| 1 | MS 0328 | L. S. Weichman | 2612 |
| 1 | MS 0328 | P. A. Smith | 2612 |
| 1 | MS 0328 | D. M. Berry | 2612 |
| 1 | MS 0328 | J. W. Bonahoom | 2612 |
| 1 | MS 0328 | C. F. Briner | 2612 |
| 1 | MS 0328 | M. H. Cannell | 2612 |
| 1 | MS 0328 | W. C. Curtis III | 2612 |
| 1 | MS 0328 | L. D. Daigle | 2612 |
| 1 | MS 0328 | L. G. Gragg | 2612 |
| 1 | MS 0328 | S. W. Green | 2612 |
| 1 | MS 0328 | K. R. Griego | 2612 |
| 1 | MS 0328 | W. R. Holiday | 2612 |
| 1 | MS 0328 | D. R. Humphreys | 2612 |
| 1 | MS 0328 | G. E. Logue | 2612 |
| 1 | MS 0328 | R. S. McEntire | 2612 |
| 1 | MS 0328 | M. J. Retter | 2612 |
| 1 | MS 0328 | J. T. Sackos | 2612 |
| 1 | MS 0328 | R. N. Shagam | 2612 |
| 1 | MS 0328 | S. R. Vigil | 2612 |
| 1 | MS 0328 | D. J. Zimmerer | 2612 |
| 1 | MS 0329 | D. A. Hoke | 2614 |
| 1 | MS 0311 | J. W. Hole | 2616 |
| 1 | MS 0311 | G. R. Lyons | 2616 |
| 1 | MS 1110 | D. E. Womble | 9214 |
| 1 | MS 1110 | L. A. Romero | 9214 |
| 1 | MS 1453 | S. M. Harris | 02553 |
| 1 | MS 9018 | Central Technical Files 8945-1 | |
| 2 | MS 0899 | Technical Library 9616 | |
| 1 | MS 06212 | Review & Approval Desk 9612 | |
| | | for DOE/ OSTI | |